Impact production of secondary electronic excitations in insulators: Multiple-parabolic-branch band model

A. N. Vasil'ev, Y. Fang, and V. V. Mikhailin
Physics Faculty, Moscow State University, Moscow 119899, Russia
(Received 17 June 1998; revised manuscript received 1 April 1999)

Analytic expressions for threshold energies and rates of electron-hole pair and exciton productions by electron impact in wide-gap insulators are given within a multiple-parabolic-branch band model which goes beyond the single-parabolic-branch model. The analysis is based on the polarization approximation. Due to the transition between the different branches, the thresholds are significantly lower than those for the single-parabolic-branch band model, and the exponents of power laws of the partial production rates are higher by 1. The interaction between components of the electron-hole pairs reduces exponents by 0.5 for both band models; an exciton reduces them by 1.5. The account for inelastic scattering with phonon emission can explain the shift of an experimentally observed threshold to higher energies. The calculated threshold of exciton production for solid Xe is in good agreement with the experimental one. [S0163-1829(99)01331-4]

I. INTRODUCTION

Electron inelastic scattering of energetic electrons is of fundamental importance in the processes of interactions of high-energy quanta with condensed matter. This scattering results in impact production of secondary electronic excitations, which is revealed in ''photon multiplication'' effect in luminescence excited by VUV photons,[1,2] whereas the cascade of such elementary acts determines the total number of electronic excitations in the scintillation process.[3] Threshold and rate are the most important characteristics of the production.

The simplest expressions for them with an allowance for energy and momentum conservation are obtained within the single-parabolic-branch band (SPBB) model of an insulator for both conduction and valence bands. For electron-hole pair production, the threshold energy is[4]

$$E_{\rm th}^{e\text{-}h}=(1+\mu)E_g, \tag{1}$$

where E_g is the gap, $\mu=m_e/(m_e+m_h)$, m_e and m_h are the effective masses of an electron and a hole, respectively, and the production rate near the threshold is[5,6]

$$W_{e\text{-}h}(E_1)\propto(E-E_{\rm th}^{e\text{-}h})^2, \tag{2}$$

where E is the kinetic energy of the initial electron. For Wannier-Mott exciton production, the threshold is[7]

$$E_{\rm th}^{\rm ex}=(1+\mu)E_{\rm ex}, \tag{3}$$

where $E_{\rm ex}$ is the exciton energy for state $n=1$, and the production rate near the threshold will be obtained below as

$$W_{\rm ex}(E)\propto\sqrt{E-E_{\rm th}^{\rm ex}}. \tag{4}$$

Beyond the SPBB model, theoretical research was conducted in two directions: real-band Monte Carlo calculations[8–13] and model-band analytic approaches.[14,15] All these calculations were made for semiconductors.

For impact production in wide-gap insulators, where the kinetic energy of the initial electron is about 10 eV, the SPBB model cannot be applied although it is valid for narrow-gap semiconductors. Moreover, the exciton effect in the threshold plays a crucial role in insulators. Recent experiment presented a vivid threshold for the secondary exciton production by a primary photoelectron after the absorption of photons in solid Xe.[16] The observed threshold energy is remarkably lower than that given by Eq. (3).

In this paper we present a multiple-parabolic-branch band (MPBB) model for the conduction band and give analytic expressions for threshold energies and rates of production of e-h pairs and excitons by electron impact in wide-gap insulators. The analysis is based on the polarization approximation.[7] Section II describes the MPBB model. The polarization approximation is presented in Sec. III. Some general expressions of production rates are given in Sec. IV. Thresholds and rates are calculated in Sec. V and Sec. VI, respectively. Conclusions are made in Sec. VII.

II. MULTIPLE-PARABOLIC-BRANCH BAND MODEL

In wide-gap insulators, the conduction band at energies about 10 eV above its bottom can be described approximately as a set of free-electron parabolic bands with effective mass $m_e=m_0$ shifted in wave-vector space by vectors $\boldsymbol{G}$ which are a superposition of reciprocal-lattice constants $\boldsymbol{b}_i$ with integer coefficients: $\boldsymbol{G}=n_1\boldsymbol{b}_1+n_2\boldsymbol{b}_2+n_3\boldsymbol{b}_3$. This representation corresponds to extended Brillouin zones Ω_∞. When only the first Brillouin zone Ω_B is considered, $\boldsymbol{G}$ identifies the branch of the dispersion law. The general form for dispersion laws is

$$E_e(\boldsymbol{k})=\frac{\hbar^2\boldsymbol{k}^2}{2m_e},\quad \boldsymbol{k}\in\Omega_\infty,\quad \text{or}\quad E_e^{\boldsymbol{G}}(\boldsymbol{k})=\frac{\hbar^2(\boldsymbol{k}-\boldsymbol{G})^2}{2m_e},\quad \boldsymbol{k}\in\Omega_B, \tag{5}$$

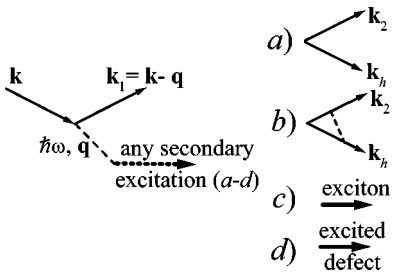

FIG. 1. Schematic representation of impact production of electron-hole pairs without (a) and with (b) interaction, excitons (c), and defect excitations (d).

where the energy origin is at the bottom of the conduction band. Thus any state in the conduction band is determined uniquely by $\boldsymbol{k}$ and $\boldsymbol{G}$. If the relaxation over quasimomentum is much faster than the relaxation over energy, the wave vector is a poor quantum number and it is convenient to use the following reduced description: energy E and branch number $\boldsymbol{G}$.

For simplicity, the spherical effective mass m_h is used for holes in the valence band:

$$E_h(\boldsymbol{k}) = \frac{\hbar^2 \boldsymbol{k}^2}{2m_h} + E_g, \quad \boldsymbol{k} \in \Omega_B. \tag{6}$$

The width of such a valence band is equal to $E_v = \hbar^2 (k_{B,\max})^2/2m_h$, where $k_{B,\max}$ is the greatest distance between the Γ point and the boundary of the Brillouin zone. In this model the initial electron can be scattered not only from the same branch as in the SPBB model, but also from branch $\boldsymbol{G}$ to branch $\boldsymbol{G}_1 \neq \boldsymbol{G}$, which is equivalent to the ''umklapp'' process.

For electron energies less than $\hbar^2 (k_{B,\min})^2/2m_e$, where $k_{B,\min}$ is the nearest distance between the Γ point and the boundary of the Brillouin zone, there is only one branch with $\boldsymbol{G}=\boldsymbol{0}$. Thus in the scattering threshold region, the transition resulting in the creation of secondary excitations from the only branch of the valence band can be restricted to the branch with $\boldsymbol{G}=\boldsymbol{0}$ in the conduction band.

III. POLARIZATION APPROXIMATION

We use the formulation of the polarization approximation given in Ref. 7. This approach allows us to regard the scattering process as emission of a virtual longitudinal photon followed by its absorption in the media. Since the absorption of such a photon can be described in terms of the energy loss function, we can take into account all processes contributing to $\mathrm{Im}[-\varepsilon^{-1}(\omega,\boldsymbol{q})]$, where $\varepsilon(\omega,\boldsymbol{q})$ is the dielectric function with account for spatial dispersion. Different processes of e-e scattering with the production of new electronic excitations are plotted in Fig. 1. In this approximation, the impact production rate for the initial electron with energy E is given as[7]

$$W_e(E) = \frac{V}{(2\pi)^3} \int d\omega \int_{\Omega_B} d\boldsymbol{q}\, \mathrm{Im}\left[-\frac{1}{\varepsilon(\omega,\boldsymbol{q})}\right] \times M_{\boldsymbol{q}}^{ee}(E, E-\hbar\omega)\rho(E-\hbar\omega), \tag{7}$$

where $\hbar\omega$ and $\hbar\boldsymbol{q}$ are the energy and the momentum transfer (of virtual longitudinal photon), respectively. ρ is the electron density of states and $M_{\boldsymbol{q}}^{ee}(E, E-\hbar\omega)$ is the e-e interaction matrix element.

For impact production of the e-h pair without account of the interaction between their components, this expression can be deduced from Fermi's golden rule. For the initial electron with wave vector $\boldsymbol{k}$ in the branch $\boldsymbol{G}$, we have

$$W_e(\boldsymbol{k},\boldsymbol{G}) = \frac{2\pi}{\hbar}\left(\frac{V}{8\pi^3}\right)^3 \sum_{\boldsymbol{G}_1,\boldsymbol{G}_2} \int_{\Omega_B}\int_{\Omega_B}\int_{\Omega_B} d\boldsymbol{k}_1 d\boldsymbol{k}_2 d\boldsymbol{k}_h \times |M(\boldsymbol{k},\boldsymbol{G};\boldsymbol{k}_1,\boldsymbol{G}_1;\boldsymbol{k}_2,\boldsymbol{G}_2;\boldsymbol{k}_h)|^2 \times \delta[E_e^{\boldsymbol{G}}(\boldsymbol{k}) - E_e^{\boldsymbol{G}_1}(\boldsymbol{k}_1) - E_e^{\boldsymbol{G}_2}(\boldsymbol{k}_2) - E_h(\boldsymbol{k}_h)], \tag{8}$$

where the integration is performed over moments of the scattered ($\boldsymbol{k}_1$) and the secondary ($\boldsymbol{k}_2$) electron and the hole ($\boldsymbol{k}_h$), and the summation covers different branches of the scattered ($\boldsymbol{G}_1$) and the secondary ($\boldsymbol{G}_2$) electrons. The exchange is not considered. The matrix element is[4]

$$|M(\boldsymbol{k},\boldsymbol{G};\boldsymbol{k}_1,\boldsymbol{G}_1;\boldsymbol{k}_2,\boldsymbol{G}_2;\boldsymbol{k}_h)|^2 = \frac{1}{V^2}\left(\frac{e^2}{\varepsilon_0|\varepsilon|}\right)^2 \frac{I_{ee}^2(\boldsymbol{k},\boldsymbol{G};\boldsymbol{k}_1,\boldsymbol{G}_1) I_{eh}^2(\boldsymbol{k}_2,\boldsymbol{G}_2;\boldsymbol{k}_h)}{\boldsymbol{q}^4} \times \sum_{\boldsymbol{G}'} \delta_{\boldsymbol{k},\boldsymbol{k}_1+\boldsymbol{k}_2+\boldsymbol{k}_h-\boldsymbol{G}'}, \tag{9}$$

where $\boldsymbol{q}$ is equal to combinations $\boldsymbol{k}-\boldsymbol{k}_1$ and $\boldsymbol{k}_2+\boldsymbol{k}_h$ reduced to the first Brillouin zone by $\boldsymbol{G}'$, and I_{ee} and I_{eh} are overlap integrals of periodic factors of Bloch functions.

According to the note mentioned in Sec. II, we use electron energy E instead of wave vector $\boldsymbol{k}$ in order to characterize an electron. Thus $W_e(E)$ is obtained by averaging over all initial states with $\boldsymbol{k}$ and $\boldsymbol{G}$ having energy $E = E_e^{\boldsymbol{G}}(\boldsymbol{k})$:

$$W_e(E) = \frac{V}{(2\pi)^3}\frac{1}{\rho(E)} \sum_{\boldsymbol{G}} \int_{\Omega_B} d\boldsymbol{k}\, \delta[E - E_e^{\boldsymbol{G}}(\boldsymbol{k})] W_e(\boldsymbol{k},\boldsymbol{G}), \tag{10}$$

where

$$\rho(E) = \frac{V}{(2\pi)^3} \sum_{\boldsymbol{G}} \int_{\Omega_B} d\boldsymbol{k}\, \delta[E - E_e^{\boldsymbol{G}}(\boldsymbol{k})] = \frac{V}{(2\pi)^3} \times \int_{\Omega_\infty} d\boldsymbol{k}\, \delta[E - E_e(\boldsymbol{k})]. \tag{11}$$

If we define an e-e interaction matrix element

$$M_{\boldsymbol{q}}^{ee}(E,E-\hbar\omega)=\frac{1}{4\pi^3}\frac{e^2}{\varepsilon_0}\frac{1}{|\boldsymbol{q}|^2\rho(E)\rho(E-\hbar\omega)}\times\sum_{\boldsymbol{G},\boldsymbol{G}_1,\boldsymbol{G}'}\int_{\Omega_B}d\boldsymbol{k}\int_{\Omega_B}d\boldsymbol{k}_1 I_{ee}^2(\boldsymbol{k},\boldsymbol{G};\boldsymbol{k}_1,\boldsymbol{G}_1)\times\delta[E-E_e^{\boldsymbol{G}}(\boldsymbol{k})]\delta[E-\hbar\omega-E_e^{\boldsymbol{G}_1}(\boldsymbol{k}_1)]\times\delta(\boldsymbol{k}-\boldsymbol{k}_1-\boldsymbol{q}-\boldsymbol{G}'),\tag{12}$$

describing the inelastic scattering of the initial electron with energy E to the states with energy $E-\hbar\omega$, and the imaginary part of the dielectric function for the e-h process

$$\varepsilon_2(\omega,\boldsymbol{q})=\frac{1}{8\pi^2}\frac{e^2}{\varepsilon_0}\frac{1}{q^2}\sum_{\boldsymbol{G}_2,\boldsymbol{G}'}\int_{\Omega_B}d\boldsymbol{k}_2\int_{\Omega_B}d\boldsymbol{k}_h I_{eh}^2(\boldsymbol{k}_2,\boldsymbol{G}_2;\boldsymbol{k}_h)\times\delta[\hbar\omega-E_e^{\boldsymbol{G}_2}(\boldsymbol{k}_2)-E_h(\boldsymbol{k}_h)]\delta(\boldsymbol{q}-\boldsymbol{k}_2-\boldsymbol{k}_h+\boldsymbol{G}'),\tag{13}$$

describing the transition from the valence band with energy $E_h(\boldsymbol{k}_h)$ to the conduction band with energy $E_e^{\boldsymbol{G}_2}(\boldsymbol{k}_2)$ as the response of the medium on the excitation, we can obtain Eq. (7). Since the bottom part of the electron band belongs to the $\boldsymbol{G}=\boldsymbol{0}$ branch, we can use only one corresponding term. The indexes in Eqs. (12) and (13) correspond to those in Eq. (9).

Equation (7) is a more general expression than Eq. (8). It also describes the production of excitons and other secondary electron excitations. With this equation the e-e and e-h processes in impact production can be treated separately.

IV. GENERAL EXPRESSIONS WITHIN THE MPBB MODEL

A. e-e matrix element and rate expression

The overlap integral of periodic factors of Bloch functions for states in the same branch in the conduction band can be estimated as $I_{ee}^2(\boldsymbol{k},\boldsymbol{G};\boldsymbol{k}_1,\boldsymbol{G}_1=\boldsymbol{G})\approx 1$. Another situation occurs for the overlap integral for bands with different $\boldsymbol{G}$. In this case, two periodic functions should be orthogonal for $\boldsymbol{k}_1=\boldsymbol{k}$ and $I_{ee}(\boldsymbol{k},\boldsymbol{G};\boldsymbol{k}_1=\boldsymbol{k},\boldsymbol{G}_1)=0$. In general, the overlap integral for free electrons is the following:

$$I_{ee}^2(\boldsymbol{k},\boldsymbol{G};\boldsymbol{k}_1,\boldsymbol{G}_1)=\frac{|\boldsymbol{k}-\boldsymbol{k}_1|^2}{|\boldsymbol{k}-\boldsymbol{G}-\boldsymbol{k}_1+\boldsymbol{G}_1|^2}=\frac{\boldsymbol{q}^2}{|\boldsymbol{q}+\boldsymbol{Q}|^2},$$

where $\boldsymbol{Q}=\boldsymbol{G}_1-\boldsymbol{G}$ is the shift between the parabolic branches in reciprocal space. Inserting this expression into Eq. (12) results in changing the q^2 factor in the denominator by $|\boldsymbol{q}+\boldsymbol{Q}|^2$. Thus the singularity q^{-2} disappears. The inaccuracy of this expression will not affect the threshold behavior, which, as will be shown below, depends mainly on the density-of-states factors.

The substitution of this expression into Eq. (12) converts sums over $\boldsymbol{G}$ and integration over Ω_B into integration over Ω_∞:

$$M_{\boldsymbol{q}}^{ee}(E,E-\hbar\omega)=\frac{1}{4\pi^3}\frac{e^2}{\varepsilon_0}\frac{1}{\rho(E)\rho(E-\hbar\omega)}\times\sum_{\boldsymbol{Q}}\int_{\Omega_\infty}d\boldsymbol{k}\int_{\Omega_\infty}d\boldsymbol{k}_1\frac{1}{|\boldsymbol{q}+\boldsymbol{Q}|^2}\times\delta[E-E_e(\boldsymbol{k})]\delta[E-\hbar\omega-E_e(\boldsymbol{k}_1)]\times\delta(\boldsymbol{k}-\boldsymbol{k}_1-\boldsymbol{q}-\boldsymbol{Q})=\sum_{\boldsymbol{Q}}M_{\boldsymbol{q}+\boldsymbol{Q}}^{ee,\mathrm{SPBB}}(E,E-\hbar\omega).\tag{14}$$

The integration of Eq. (14) results in

$$M_{\boldsymbol{q}}^{ee,\mathrm{SPBB}}(E,E-\hbar\omega)=\frac{m_e^2e^2}{2\pi^2\varepsilon_0\hbar^4}\times\frac{1}{\rho(E)\rho(E-\hbar\omega)}\frac{1}{q^3}\Theta(\omega,|\boldsymbol{q}|,E).\tag{15}$$

Factor Θ equals 1 if the scattering process with emission of a photon with energy $\hbar\omega$ and wave vector $\boldsymbol{q}$ is allowed by the combination of energy and momentum conservation laws:

$$\Theta(\omega,q,E)=\theta[\omega-\omega^-(E,q)]-\theta[\omega-\omega^+(E,q)]=\theta[q-q^-(E,\omega)]-\theta[q-q^+(E,\omega)],$$

with $\hbar\omega^-=0$, $\hbar\omega^+(E,q)=E-(\hbar q-\sqrt{2m_eE})^2/2m_e$, and $\hbar q^\pm(E,\omega)=\sqrt{2m_eE}\pm\sqrt{2m_e(E-\hbar\omega)}$. The limits for q are not dependent on Q and are the same as were given in Refs. 17–19 for the SPBB model. With the dispersion law given by Eq. (5), Eq. (11) results in

$$\rho(E)=\frac{V(2m_e)^{3/2}}{4\pi^2\hbar^3}\sqrt{E}.\tag{16}$$

Inserting Eqs. (14), (15), and (16) into Eq. (7), we obtain

$$W_e(E)=\sum_{\boldsymbol{Q}}W_{\boldsymbol{Q}}(E)=\sum_{|Q|}n_QW_{|Q|}(E),\tag{17}$$

where n_Q is the number of nodes with the same $|\boldsymbol{Q}|$ in reciprocal space, and

$$W_Q(E)=\frac{e^2}{8\pi^3\varepsilon_0\hbar}\sqrt{\frac{m_e}{2E}}\int d\omega\int\frac{d\boldsymbol{q}}{|\boldsymbol{q}+\boldsymbol{Q}|^3}\times\mathrm{Im}\left[-\frac{1}{\varepsilon(\omega,\boldsymbol{q})}\right]\Theta(\omega,|\boldsymbol{q}+\boldsymbol{Q}|,E).\tag{18}$$

When we take into account only the term with $\boldsymbol{Q}=\boldsymbol{0}$, Eq. (18) is reduced to the well-known formula obtained within the SPBB model for the electron gas[20] and for condensed matter[21] and serves as a basic formula to treat the inelastic scattering of electron in condensed matter.[17–19,22]

B. ε_2 and rate expression

Equation (13) describes ε_2 for the case of electron-hole excitation without interaction between these particles. When this interaction is taken into account, ε_2 has a more complicated form. The expression for ε_2 in the case of the Wannier-Mott exciton with $\boldsymbol{q}=\mathbf{0}$ was obtained in Ref. 24. The extension of this formula to $\boldsymbol{q}\neq\mathbf{0}$ can be obtained for nondegenerated bands using a transition to the center-of-mass system. In this case, ε_2 is the function of $\hbar\omega - E_g - \hbar^2 q^2/2(m_e+m_h)$ for energies $\hbar\omega$ less than $E_g + \hbar^2 k_{\min,B}^2/2m_e$ (when only the lowest band in the conduction band is taken into account). Assuming that $|\varepsilon|^2$ varies slower than ε_2, we can write a general expression for both exciton and e-h pair production as (see the Appendix)

$$W_Q(E)=\frac{e^2}{4\pi^2\varepsilon_0}\,\frac{\sqrt{2m_e}}{3|\varepsilon|^2\hbar\mu}\,\frac{1}{\sqrt{E_Q E}}\int d\omega\,\varepsilon_2(\omega,0)\times\left[\frac{\Delta_-^{3/2}\theta(\Delta_-)}{(\sqrt{E}+\mu\sqrt{E_Q})^2}-\frac{\Delta_+^{3/2}\theta(\Delta_+)}{(\sqrt{E}-\mu\sqrt{E_Q})^2}\right], \quad (19)$$

where

$$\Delta_\pm=(\sqrt{E}\mp\mu\sqrt{E_Q})^2-(1+\mu)(\hbar\omega+\mu E_Q) \quad (20)$$

with $E_Q=\hbar^2Q^2/2m_e$.

The expression for $Q=0$ near the threshold can be reduced from Eq. (19) by taking the limit as follows:

$$W_0(E)=\lim_{Q\to 0}W_Q(E)=\frac{\sqrt{2}e^2\sqrt{m_e}}{2\pi^2\varepsilon_0|\varepsilon|^2\hbar}\,\frac{1}{E}\times\int d\omega\,\varepsilon_2(\omega,0)\sqrt{E-(1+\mu)\hbar\omega}\times\theta[E-(1+\mu)\hbar\omega]. \quad (21)$$

V. THRESHOLDS

The integrands in Eqs. (19) and (21) are equal to zero if the corresponding θ functions are equal to zero (these functions set an upper limit in the integrals) or $\varepsilon_2(\omega,0)$ is equal to zero in the transparency region (this threshold of the absorption defines the lower limit in the integrals). The threshold energy can be determined from the coincidence of these two limits. The expressions of thresholds for exciton and e-h pair production have the same form, which can be determined by substituting $\hbar\omega=E_d$ (where the notation E_d is used for the photon absorption threshold for the creation of corresponding excitations, $E_d=E_g$ for e-h pair and $E_d=E_{\rm ex}$ for exciton) into $\Delta_\pm=0$, i.e.,

$$(\sqrt{2m_eE_{\rm th,}{}_Q^{\pm}}\mp\mu\hbar Q)^2=(1+\mu)(2m_eE_d+\mu\hbar^2Q^2), \quad (22)$$

which gives the lower and upper thresholds corresponding to Δ_- and Δ_+ as

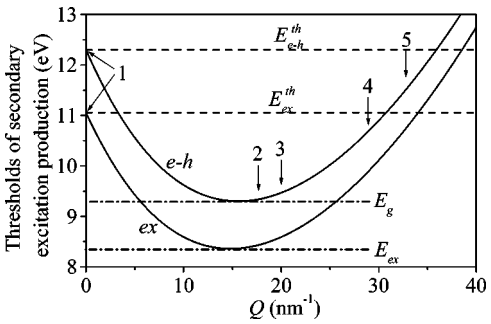

FIG. 2. Lower thresholds of impact production of Wannier-Mott $n=1$ exciton and e-h pair vs Q for solid Xe calculated by Eq. (23) with parameters given in the text and Table I.

$$E_{\rm th,}{}_Q^{\pm}=E_{\rm th}^0\pm 2\mu\sqrt{E_Q}\sqrt{(1+\mu)(E_d+\mu E_Q)}+\mu(1+2\mu)E_Q, \quad (23)$$

where

$$E_{\rm th}^0=(1+\mu)E_d \quad (24)$$

is the threshold for $Q=0$.

In comparison with the SPBB model, which is the special case here when $Q=0$, the threshold has two values (due to the transition to the other branch of the bands): the upper threshold is always larger than $E_{\rm th}^0$, which has less of an effect on the rate in the threshold, while the lower threshold can be significantly lower than $E_{\rm th}^0$. The lowest threshold $E_{\rm th,}{}_Q^{-}=E_d$ can be achieved if $\hbar Q=\sqrt{2m_eE_d}$. In this case, the vertical transition from the valence band to the conduction band, like that in the photon absorption, becomes possible due to the transition of the initial electron from the branch with $\hbar G=\sqrt{2m_eE_d}$ to the branch $G=0$, allowing for the momentum conservation. The same reduction of the threshold was obtained numerically[8] and analytically[23] for e-h pair production in silicon due to the multivalley conduction-band structure, which is similar to the MPBB model here. For solid Xe the lower threshold versus Q calculated by Eq. (23) for exciton and e-h productions is plotted in Fig. 2 with the parameter of the fcc lattice constant $a=0.62$ nm and the band parameters[16] $E_{\rm ex}=8.359$ eV, $E_g=9.3$ eV, $m_e=m_0$, $m_h=2.1m_0$. The numbers in Fig. 2 correspond to the transitions to the branch with $G=0$ from different branches, which parameters and respective lower thresholds are shown in Table I.

The transition of the initial electron from the nearest branch with $Q=2\pi\sqrt{3}/a$ has the lowest threshold for exci-

TABLE I. Multiple-branch parameters of solid Xe and associated lower thresholds for five different branches with the band-structure parameters given in the text.

	1	2	3	4	5
Q	0	$2\pi\sqrt{3}/a$	$4\pi/a$	$4\pi\sqrt{2}/a$	$2\pi\sqrt{11}/a$
n_Q	1	8	6	12	24
$E_{\rm th}^{\rm ex}$ (eV)	11.06	8.43	8.62	9.84	10.95
$E_{\rm th}^{e\text{-}h}$ (eV)	12.30	9.33	9.49	10.64	11.72

ton production $E_{\rm th}^{\rm ex}=8.43$ eV, which is in good agreement with the threshold $E_{\rm th}^{\rm ex}=8.45$ eV determined by the experiment of Ref. 16.

VI. PRODUCTION RATES NEAR THRESHOLDS

If $\varepsilon_2(\omega,0)$ defined in Eq. (13) is determined, the production rate can be obtained using Eq. (19) and Eq. (21). Function ε_2 with $\boldsymbol{q}=\mathbf{0}$ can be easily obtained from an experiment. Ratio I_{eh}^2/q^2 near the threshold can be roughly estimated by the $\boldsymbol{k}\cdot\boldsymbol{p}$ method as[4]

$$\frac{I_{eh}^2}{q^2}=\frac{\hbar^2}{m_eE_g}. \tag{25}$$

Then $\varepsilon_2(\omega,\boldsymbol{q})$ can be calculated using Eq. (13) for dispersion laws given in Eqs. (5) and (6) without taking interparticle interaction into account:

$$\varepsilon_2(\omega,\boldsymbol{q})=C_\varepsilon\sqrt{\hbar\omega-E_g-\hbar^2q^2/2(m_e+m_h)}\times\theta[\hbar\omega-E_g-\hbar^2q^2/2(m_e+m_h)], \tag{26}$$

where

$$C_\varepsilon=\frac{e^2}{4\pi\varepsilon_0\hbar}\,\frac{1}{m_eE_g}\left(\frac{2m_em_h}{m_e+m_h}\right)^{3/2}.$$

Allowance for e-h interaction results in the above-mentioned extension of Elliott's formula:[24]

$$\varepsilon_2(\omega,\boldsymbol{q})=C_\varepsilon\left[\sum_n\frac{4\pi(\mathrm{Ry}^*)^{3/2}}{n^3}\delta[\hbar\omega-E_g+\mathrm{Ry}^*/n^2-\hbar^2q^2/2(m_e+m_h)]+2\pi\sqrt{\mathrm{Ry}^*}\frac{\theta[\hbar\omega-E_g-\hbar^2q^2/2(m_e+m_h)]}{1-\exp\{-2\pi\sqrt{\mathrm{Ry}^*/[\hbar\omega-E_g-\hbar^2q^2/2(m_e+m_h)]}\}}\right], \tag{27}$$

where $\mathrm{Ry}^*=E_g-E_{\rm ex}$. This formula describes the production of both bound exciton states [discreet sum in Eq. (27)] and separated electron-hole states [last term in Eq. (27)]. Allowance for e-h interaction changes the behavior of ε_2 near E_g from square root law to constant value without any singularity at E_g [for energies above $E_g+\hbar^2q^2/2(m_e+m_h)$ the denominator of the last term in Eq. (27) is equal to 1]. Only for energies about 2 Ry* above the threshold can one neglect e-h interaction and Eq. (27) asymptotically goes over into Eq. (26).

From Eq. (27) we have ε_2 for three special cases:

For exciton $n=1$,

$$\varepsilon_2(\omega,\boldsymbol{q})=C_\varepsilon 4\pi(\mathrm{Ry}^*)^{3/2}\delta[\hbar\omega-E_{\rm ex}-\hbar^2q^2/2(m_e+m_h)]; \tag{28}$$

for e-h pairs with interaction,

$$\varepsilon_2(\omega,\boldsymbol{q})=C_\varepsilon 2\pi(\mathrm{Ry}^*)^{1/2}\theta[\hbar\omega-E_g-\hbar^2q^2/2(m_e+m_h)]. \tag{29}$$

For e-h pairs without interaction, the case corresponds to Eq. (26).

With Eq. (20) and Eq. (22), $\Delta_\pm$ can be expressed as

$$\Delta_\pm=A_\pm+(1+\mu)(E_d-\hbar\omega),$$

where

$$A_\pm=E-E_{{\rm th},Q}^{\pm}\mp2\mu\sqrt{E_Q}(\sqrt{E}-\sqrt{E_{{\rm th},Q}^{\pm}}). \tag{30}$$

Using these definitions and substituting Eq. (26) and Eqs. (28) and (29) into Eq. (19), we obtain a formula for the rate of impact production of the secondary electron excitations,

$$W_Q(E)=\frac{\beta}{\tau_0}\,\frac{(\mathrm{Ry}^*)^{3-\alpha}}{|\varepsilon|^2E_g\sqrt{E_QE}}\left[\frac{A_-^\alpha\,\theta(E-E_{{\rm th},Q}^-)}{(\sqrt{E}+\mu\sqrt{E_Q})^2}-\frac{A_+^\alpha\,\theta(E-E_{{\rm th},Q}^+)}{(\sqrt{E}-\mu\sqrt{E_Q})^2}\right] \tag{31}$$

with

$$\frac{1}{\tau_0}=\left(\frac{e^2}{4\pi\varepsilon_0}\right)^2\frac{m_e}{\hbar^3}=4.14\times10^{16}\ \ \mathrm{s}^{-1}.$$

TABLE II. Parameters for Eqs. (31) and (33) for different types of secondary excitations.

	α	β	α_0	β_0
$n=1$ exciton	1.5	$\frac{16(1-\mu)^{3/2}}{3\mu}$	0.5	$32(1-\mu)^{3/2}$
e-h pair with interaction	2.5	$\frac{16(1-\mu)^{3/2}}{15\mu(1+\mu)}$	1.5	$\frac{32(1-\mu)^{3/2}}{3(1+\mu)}$
e-h pair without interaction	3	$\frac{1}{12\mu}\left(\frac{1-\mu}{1+\mu}\right)^{3/2}$	2	$\left(\frac{1-\mu}{1+\mu}\right)^{3/2}$

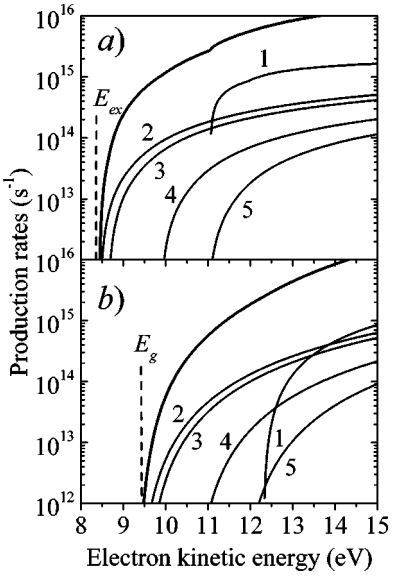

FIG. 3. Rates of impact production of (a) Wannier-Mott exciton and (b) *e*-*h* pairs with interaction for solid Xe. The thin lines are partial rates with the numbers indicating the different branches. The thick lines are their total rates. The calculation parameters are given in the text and Table I with $|\varepsilon|^2 \approx 10$.

Values of parameters α and β for $n=1$ exciton and *e*-*h* pairs with and without interaction are shown in Table II. For $\boldsymbol{Q} \neq \boldsymbol{0}$, two thresholds are well separated, and only $E^{-}_{\mathrm{th},Q}$ should be taken into account. The behavior of $W_Q(E)$ becomes much more simple:

$$W_Q(E)=\frac{\beta}{\tau_0}\frac{(\mathrm{Ry}^*)^{3-\alpha}}{|\varepsilon|^2 E_g E^{-}_{\mathrm{th},Q}\sqrt{E_Q E^{-}_{\mathrm{th},Q}}}\left[1+\mu\sqrt{\frac{E_Q}{E^{-}_{\mathrm{th},Q}}}\right] \times (E-E^{-}_{\mathrm{th},Q})^{\alpha}\theta(E-E^{-}_{\mathrm{th},Q}). \quad (32)$$

Substituting Eq. (26) and Eqs. (28) and (29) into Eq. (21), or taking the limit in Eq. (31), we obtain the formula for impact production of secondary electron excitations for $Q=0$ as

$$W_0(E)=\frac{\beta_0}{\tau_0}\frac{(\mathrm{Ry}^*)^{2-\alpha_0}}{|\varepsilon|^2 E_g E}(E-E^0_{\mathrm{th}})^{\alpha_0}, \quad (33)$$

with E^0_{th} defined in Eq. (24) and parameters α_0 and β_0 shown in Table II. For an *e*-*h* pair without interaction we obtain the Keldysh formula Eq. (2). For excitons, Eq. (33) corresponds to Eq. (4) mentioned in the Introduction.

A similar change of the softness for the impact production rate of an *e*-*h* pair in semiconductors from power 2 (given by the SPBB model) to higher power (for the complicated conduction-band structure) was obtained analytically (to power 3)[14,15] and numerically.[9,11] This softness is due to the anisotropy of the *e*-*e* transition processes with $\boldsymbol{Q}\neq\boldsymbol{0}$ as well as the decrease of the density of possible final states for scattering process.

The results for partial impact production rates [Eq. (31) and Eq. (33)] and total rate [Eq. (17)] are plotted in Fig. 3. The partial rate $W_0(E)$ is the largest one for high energies (curve 1). The partial rate decreases when Q increases due to the growth of the mean distance between the associated two branches in the reciprocal space. The interesting step structure in the total rate associated with the discrete summation of the partial rates was also obtained for the impact ionization rates in semiconductors with more real conduction-band structures both analytically[15] and numerically.[9]

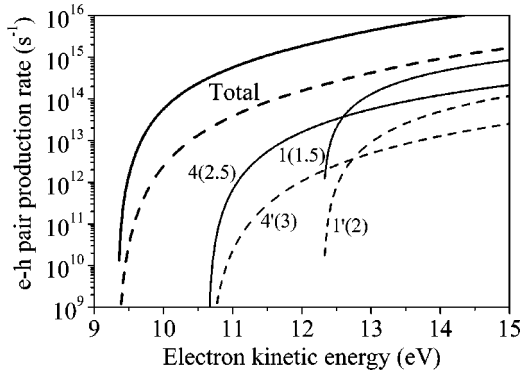

FIG. 4. Rates of impact production of *e*-*h* pairs for solid Xe. Solid and dashed lines are the rates for *e*-*h* pairs with and without interaction, respectively. The thin lines are partial rates with the numbers indicating the different branches and the numbers in parentheses are exponents of the power laws. The thick lines are total rates. The calculation parameters are given in the text and Table I with $|\varepsilon|^2 \approx 10$.

Figure 4 presents the comparison between rates for production of *e*-*h* pairs with and without interaction. The interaction between an electron and a hole from secondary excitation reduces exponents by 0.5 (see Table II).

Strong inelastic scattering of electrons results in the creation of excitations of two types: excitons in any bound states ($n=1,\ldots,\infty$) and electron-hole pairs in continuum states. The yield of excitons in this scattering process

$$R(E)=W^{\mathrm{ex}}(E)/[W^{\mathrm{ex}}(E)+W^{e\text{-}h}(E)] \quad (34)$$

is plotted in Fig. 5. The yield of secondary electron-hole pairs is equal to $1-R(E)$. Equation (34) does not take into account the scattering of the secondary excitations on phonons, which can significantly redistribute excitations over

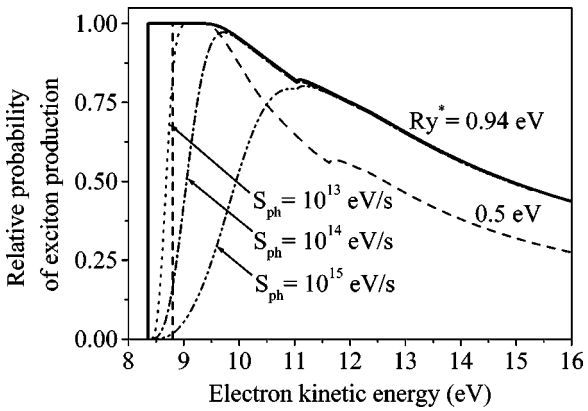

FIG. 5. The yield of secondary excitons $R(E)$ [given by Eq. (34)] for solid Xe without phonon relaxation for two values of exciton bound energies (Ry*=0.94 eV and 0.5 eV) and $R^{\mathrm{ph}}(E)$ with different rates of phonon relaxation S_{ph} [Eq. (36); Ry* =0.5 eV].

their types. An example of such phonon-assistant processes is autoionization of an exciton with relatively high total wave vector $\boldsymbol{q}$ [for the $n=1$ exciton this process is allowed for $\hbar^2q^2/2(m_e+m_h)>\mathrm{Ry}^*$].

Experimentally observed efficiency of secondary excitation production is masked by interaction with phonons in different ways. Scattering with emission of phonons can play an important role before and after the strong inelastic scattering discussed in the present paper.

Phonon emission before the scattering plays a double role. At this stage, the initial electron interacts mainly with short-wavelength phonons. In such a case, the rate of momentum relaxation seems to be higher than the rate of energy relaxation. Therefore, this emission results in randomization of wave vectors of primary electrons, and thus reduces the anisotropy of the scattering process. This randomization allows us to pass to the reduced set of quantum numbers and use only the energy to describe the initial electron (see Sec. II). But the energy relaxation due to phonon emission is also important and can significantly reduce the yield of secondary excitations in the threshold region, since this process is a competition channel of relaxation. The kinetic equation for electron energy distribution function $f(E)$ in the near-threshold region for stationary excitation of electrons with energy E_0 and intensity I can be written as

$$S_{\mathrm{ph}}(E)\frac{\partial f(E)}{\partial E}-W_e(E)f(E)+I\delta(E-E_0)=0, \qquad (35)$$

where $S_{\mathrm{ph}}(E)$ is the speed of energy losses for primary electron with energy E due to phonon emission [$S_{\mathrm{ph}}=\Sigma_\sigma W_\sigma^{\mathrm{ph}}(E)\hbar\Omega_\sigma$, $W_\sigma^{\mathrm{ph}}(E)$, and Ω_σ denote the emission rate and frequency for phonons of mode σ]. Solving this equation, we can get the probability for scattering of an electron with initial energy E_0 with the production of new electronic excitation:

$$1-\exp\left(-\int_{E_{\mathrm{th}}}^{E_0}\frac{W_e(E)dE}{S_{\mathrm{ph}}(E)}\right).$$

Near the lowest threshold $E_{\mathrm{th}}=\min(E_{\mathrm{th},Q}^-)$ we can use a power approximation of $W_e(E)\approx C(E-E_{\mathrm{th}})^\alpha$, and therefore the yield of exciton production [Eq. (34)] goes over into

$$R^{\mathrm{ph}}(E)=R(E)\left[1-\exp\left(-\frac{C(E-E_{\mathrm{th}})^{\alpha+1}}{S_{\mathrm{ph}}(E_{\mathrm{th}})}\right)\right]. \qquad (36)$$

Due to this factor the experimentally observed threshold of secondary excitation production is shifted to higher energies and becomes smooth. This effect is displayed in Fig. 5.

VII. CONCLUSION

The present study shows that simple multiple-branch dispersion law results in an essential shift in threshold energy for the production of secondary excitations. The rate of this inelastic scattering is slower than for the SPBB model. The competition with other relaxation processes shifts the experimentally observed threshold to higher energies. The analysis uses polarization approximation and results in analytic formulas for rates of impact production of secondary excitations, both of electron-hole pairs and excitons. This information is of great importance for the estimation of efficiency of energy conversion for scintillators.

ACKNOWLEDGMENTS

The support of grants RFBR 97-02-17414, RFBR-DFG 96-02-00207G, Federal Program 2.1-535, and DFG No. 436 RUS 113/437 are gratefully acknowledged. The authors would like to thank Professor G. Zimmerer for fruitful discussions.

APPENDIX

With

$$\varepsilon_2(\omega,\boldsymbol{q})=f[\hbar\omega-E_g-\hbar^2q^2/2(m_e+m_h)], \qquad (A1)$$

the integration in Eq. (18) can be carried out as

$$\begin{aligned}W_Q(E)&=C_1\int d\omega\int_{\Omega_\infty}\frac{d\boldsymbol{q}}{|\boldsymbol{q}+\boldsymbol{Q}|^3}f[\hbar\omega-E_g\\&\quad-\hbar^2q^2/2(m_e+m_h)]\Theta(\omega,|\boldsymbol{q}+\boldsymbol{Q}|,E)\\&=C_1 2\pi\int d\omega\int\frac{dq}{q}\int_{-1}^{1}dx\,f\left[\hbar\omega-E_g\right.\\&\quad\left.-\frac{\hbar^2(q^2+Q^2-2qQx)}{2(m_e+m_h)}\right]\Theta(\omega,q,E). \qquad (A2)\end{aligned}$$

By using

$$\begin{aligned}&f\left[\hbar\omega-E_g-\frac{\hbar^2(q^2+Q^2-2qQx)}{2(m_e+m_h)}\right]\\&\quad=\hbar\int d\omega' f(\hbar\omega')\delta\left[\hbar\omega'-\hbar\omega+\frac{\hbar^2(q^2+Q^2-2qQx)}{2(m_e+m_h)}\right],\end{aligned}$$

we can get

$$\begin{aligned}W_Q(E)&=C_1\frac{2\pi(m_e+m_h)}{\hbar Q}\int d\omega' f(\hbar\omega')\int\frac{dq}{q^2}\\&\quad\times\int d\omega\left\{\theta\left[\hbar\omega'-\hbar\omega+\frac{\hbar^2(q-Q)^2}{2(m_e+m_h)}\right]\right.\\&\quad\left.-\theta\left[\hbar\omega'-\hbar\omega+\frac{\hbar^2(q+Q)^2}{2(m_e+m_h)}\right]\right\}\Theta(\omega,q,E)\\&=C_1\frac{2\pi(m_e+m_h)}{\hbar Q}\int d\omega' f(\hbar\omega')\\&\quad\times\left[\int\frac{dq}{q^2}I^-(E,q,Q,\omega')-\int\frac{dq}{q^2}I^+(E,q,Q,\omega')\right],\end{aligned} \qquad (A3)$$

where

$$I^{\pm}(E,q,Q,\omega')=\int_{\omega'+(q\pm Q)^2/2(m_e+m_h)}^{E/\hbar-(\hbar q-\sqrt{2m_eE})^2/2m_e\hbar} d\omega$$

$$=\frac{-1}{2m_e\hbar}[(1+\mu)\hbar^2q^2 - 2(\sqrt{2m_eE}\mp\mu\hbar Q)\hbar q + 2m_e\hbar\omega'+\mu\hbar^2Q^2]. \quad \text{(A4)}$$

The limits of integrations over q in Eq. (A3) are roots of $I^{\pm}(E,q,Q,\omega')=0$, respectively:

$$\frac{\hbar q^{+}_{(1,2)}}{\sqrt{2m_e}}=\frac{\sqrt{E}-\mu\sqrt{E_Q}\pm\sqrt{\Delta_+}}{1+\mu} \quad \text{for} \quad I^{+}(E,q,Q,\omega') \quad \text{(A5)}$$

and

$$\frac{\hbar q^{-}_{(1,2)}}{\sqrt{2m_e}}=\frac{\sqrt{E}+\mu\sqrt{E_Q}\pm\sqrt{\Delta_-}}{1+\mu} \quad \text{for} \quad I^{-}(E,q,Q,\omega') \quad \text{(A6)}$$

with

$$\Delta_{\pm}=(\sqrt{E}\mp\mu\sqrt{E_Q})^2-(1+\mu)(\hbar\omega'+\mu E_Q)\geqslant 0. \quad \text{(A7)}$$

Integration for I^{-} over q is easily carried out as

$$\int_{q_1^-}^{q_2^-}\frac{dq}{q^2}I^{-}(E,q,Q,\omega')$$

$$=\frac{1}{\sqrt{2m_e}}\left[2\sqrt{\Delta_-}+2(\sqrt{E}+\mu\sqrt{E_Q})\ln\frac{\sqrt{E}+\mu\sqrt{E_Q}-\sqrt{\Delta_-}}{\sqrt{E}+\mu\sqrt{E_Q}+\sqrt{\Delta_-}} + (\hbar\omega'+\mu E_Q)\left(\frac{1+\mu}{\sqrt{E}+\mu\sqrt{E_Q}-\sqrt{\Delta_-}} - \frac{1+\mu}{\sqrt{E}+\mu\sqrt{E_Q}+\sqrt{\Delta_-}}\right)\right]$$

$$=\frac{1}{\sqrt{2m_e}}\left[4\sqrt{\Delta_-}+2(\sqrt{E}+\mu\sqrt{E_Q}) \times\ln\frac{\sqrt{E}+\mu\sqrt{E_Q}-\sqrt{\Delta_-}}{\sqrt{E}+\mu\sqrt{E_Q}+\sqrt{\Delta_-}}\right]. \quad \text{(A8)}$$

Near the threshold $\Delta_-\to 0$, the expansion of the logarithm in the above formula results in

$$\int_{q_1^-}^{q_2^-}\frac{dq}{q^2}I^{-}(E,q,Q,\omega')\approx 2\sqrt{\frac{2}{3}}\frac{\Delta_-^{3/2}}{\sqrt{m_e}(\sqrt{E}+\mu\sqrt{E_Q})^2}. \quad \text{(A9)}$$

Substituting Eq. (A9) and the similar expression after integrating for I^{+} into Eq. (A3), we have Eq. (19).

[1] A. Lushchik, E. Feldbach, Ch. Lushchik, M. Kirm, and I. Martinson, Phys. Rev. B **50**, 6500 (1994).
[2] A. Lushchik, E. Feldbach, R. Kink, Ch. Lushchik, M. Kirm, and I. Martinson, Phys. Rev. B **53**, 5379 (1996).
[3] V. V. Mikhailin, Nucl. Instrum. Methods Phys. Res. B **97**, 530 (1995).
[4] B. K. Ridley, *Quantum Processes in Semiconductors*, 3rd ed. (Oxford University Press, Oxford, 1993).
[5] L. V. Keldysh, Zh. Éksp. Teor. Fiz. **37**, 713 (1960) [Sov. Phys. JETP **10**, 509 (1960)].
[6] D. J. Robbins, Phys. Status Solidi B **97**, 9 (1980); **97**, 387 (1980).
[7] A. N. Vasil'ev, Nucl. Instrum. Methods Phys. Res. B **107**, 165 (1996).
[8] E. O. Kane, Phys. Rev. **159**, 624 (1967).
[9] N. Sano and A. Yoshii, Phys. Rev. B **45**, 4171 (1992).
[10] N. Sano and A. Yoshii, J. Appl. Phys. **77**, 2020 (1995).
[11] M. Stobbe, R. Redmer, and W. Schattke, Phys. Rev. B **49**, 4494 (1994).
[12] Y. Wang and K. F. Brennan, J. Appl. Phys. **75**, 313 (1994).
[13] J. Bude and K. Hess, J. Appl. Phys. **72**, 3554 (1992).
[14] A. R. Beattie, Semicond. Sci. Technol. **3**, 48 (1988).
[15] R. Thoma, H. J. Peifer, W. L. Engl, W. Quade, R. Brunetti, and C. Jacoboni, J. Appl. Phys. **69**, 2300 (1991).
[16] B. Steeg, M. Kirm, V. Kisand, S. Körding, S. Vielhauer, and G. Zimmerer, J. Low Temp. Phys. **111**, 739 (1998).
[17] J. C. Ashley and V. E. Anderson, J. Electron Spectrosc. Relat. Phenom. **24**, 127 (1981).
[18] J. C. Ashley, J. Electron Spectrosc. Relat. Phenom. **28**, 177 (1982).
[19] J. C. Ashley, J. Electron Spectrosc. Relat. Phenom. **46**, 199 (1988).
[20] R. H. Ritchie, Phys. Rev. **114**, 644 (1959).
[21] U. Fano, Phys. Rev. **103**, 1202 (1956).
[22] C. J. Powell, Surf. Sci. **44**, 29 (1974).
[23] Y. Lu and C.-T. Sah, Phys. Rev. B **52**, 5657 (1995).
[24] R. J. Elliott, Phys. Rev. **108**, 1384 (1957).